Study of one-step and two-step quench and partition heat treatments on a medium carbon high silicon alloy using dilatometry

V Kurup[1a]*, CW Siyasiya[1b], RJ Mostert[1c], J Moema[2d]

[1] Department of Material Science and Metallurgical Engineering, University of Pretoria
[2] Mintek, South Africa
Email: [a] vinod.kurup@up.ac.za, [b] charles.siyasiya@up.ac.za, [c] roelf.mostert@up.ac.za, [d] josephm@mintek.co.za

Abstract

This study evaluated the microstructural evolution in a medium carbon high silicon steel during one-step, and two-step quench and partition (Q&P) processes using dilatometry experiments. The two-step Q&P process was carried out using different quench temperatures ranging from 180 to 260 °C. In the one-step process, Q&P heat treatment samples were held isothermally for ten minutes after quenching at specified temperatures ranging between 200 and 450°C. The two-step Q&P process yielded a higher fraction of retained austenite than a one-step Q&P process. During the isothermal hold step, the volume expansion due to carbon partitioning and austenite decomposition behavior was interpreted by experimentally determined strain values. For the one-step Q&P process, the austenite decomposition kinetics above and below the M_s temperature differed, as evidenced by the JMAK parameters. The TTT diagram generated for the one-step Q & P process showed a "swing back" at a temperature of around 355°C.

Keywords: Quench and Partitioning; Dilatometry; Microstructure, Bainite

1. Introduction

Advanced high strength steels (AHSS) have been a significant driver in new steel developments for automotive applications. Their development was lead by creating multiphase structures to improve strength and elongation.[1] Quench and partition process (Q&P) is one such heat treatment proposed by Speer[2] to obtain multiphase microstructure as required for 3rd generation AHSS. The typical microstructure of Q&P processed steel consists of a martensite matrix with embedded retained austenite (RA) in film or blocky form. The key alloying elements of Q&P processed steel consists of C, Mn, Si, or Al. The addition of Mn improves hardenability, and Si is added to suppress the formation of cementite.[3] The two-step Q&P proposed by Speer based on the constraint carbon equilibrium concept[4] has four steps: (i) austenitization, (ii) quenching between M_s and M_f to obtain martensite-austenite mixture, (iii) partitioning step whereby the steel is heated to a higher temperature above M_s to facilitate carbon partitioning and (iv) final cooling to room temperature.

The dilatometric analysis of the Q&P process[5] showed that the Q&P process is more complex, with other transformations taking place along with carbon partitioning. Kim et al.[6] had observed isothermal transformation at quenching temperature. However, the nature of the transformation product was not clear. In this paper, we look into the progression of partitioning reaction, which occurs in the third stage of Q&P heat treatment during the one and two-step Q&P process. The two-step and one-step Q&P heat treatment shown in Fig1 (a) & (b) were carried out on high silicon steel at various quench temperatures to evaluate the effect of heat treatment type and quench temperature on the stabilization of RA. The kinetics of the one-step Q&P process were examined during isothermal transformation by fitting the JMAK equation.

2. Material and methods

A hot worked steel with the composition shown in Table 1 used a dilatometer to study the phase transformation and kinetics for the Q&P process. The steel was melted in an induction furnace and cast. The cast ingot was heated to a temperature of 1200°C for 3 hours. It was followed by hot forging at 900°C to 50 mm square bars and further hot rolled to a diameter of 15 mm x 30 mm long rods. These samples were cut to a diameter of 5 mm x 10 mm length for dilatometry experiments. After determining the critical temperatures A_{c1}, A_{c3}, and M_s, the alloys were subject to the two-step and one-step Q&P heat treatment as shown schematically in Figure 1(a) & (b).

Heat treatments were carried out in a Bhr 805A dilatometer. Specimens were placed between the two silica rods and heated by an induction coil under a vacuum. Helium was used as a cooling medium for quenching purposes. Different heat treatments were carried out after austenitization at 900°C for 300 s. The applied

Table 1: The chemical composition (wt. %) and critical temperatures of the investigated alloy

Element	C	Mn	Si	Al	Cr	P	S	Ti	B	M_s	A_{c1}	A_{c3}
Amount (Wt. %)	0.27	2.8	2.2	0.50	0.75	0.011	0.014	0.009	0.001	368°C	750°C	860°C
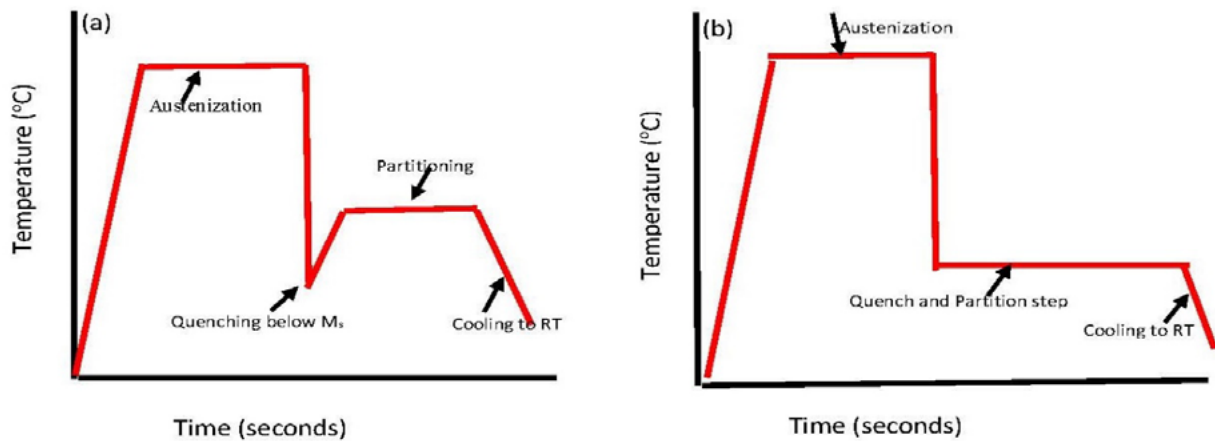
Figure 1: Schematic diagrams of the heat treatment profiles carried out in the dilatometer (a) Two-step Q&P (b) One-step Q&P

heat treatments are described as follows: (a) Direct quench to room temperature after austenitization to determine the M_s, determined as 368°C. (b) The two-step Q&P heat treatment carried above and below the optimum quench temperature Fig 1(a). The samples were quenched to the following temperatures: 180, 200, 220, 225, 240, and 260°C, then partitioning at 400°C for 200 s. (c) The isothermal treatments are referred to here as a one-step Q&P heat treatment performed above and below the M_s temperature Fig 1(b). Here the quench and partitioning process takes place at the same temperature. The dilatometry data obtained from the partitioning stage of the one-step Q&P process was analyzed using the Johnson–Mehl-Avrami-Kolmogorov (JMAK) equation:

$$f_{\alpha'} = 1 - exp(kt^n) \qquad \text{Equation 1}$$

Where f_x=fraction transformed; t=time; k=frequency factor; and n=Awrami exponent

The isothermal data was then plotted as $\ln(\ln(\frac{1}{1-f_\alpha}))$ vs. ln t. Using the least square fit method on the dilatometric data, "n" and "k" parameters of the JMAK equation were obtained. The isothermal kinetics obtained by analyzing the JMAK equation differ significantly above and below the M_s, suggesting different phases above and below M_s. The heat-treated samples were then analyzed using neutron diffraction at the Nuclear Energy Council of South Africa (NECSA). The aim was to identify the different phases present after the Q&P heat treatment. The samples were scanned in the 2θ range from 27 to 115 degrees. The diffraction patterns obtained were analyzed by the Rietveld method[7] using TOPAZ 4.2 software. The lattice parameters obtained for RA was related to its carbon content using the empirical relationship between lattice constant and composition[8] as given by equation 2:

a (γ) = 0.3556+0.00453(W_C)+0.00095(W_Mn) +0.0056(W_Al)
+0.0006 (W_Cr)-0.0002(W_Ni)   *Equation 2*

Where a(γ) = lattice parameter of austenite, and W_C, W_{MN}, W_{Al}, W_{Cr}, and W_{Ni} are the weight percent of C, Mn, Al, Cr, and Ni in the RA phase.

The heat-treated dilatometer samples were ground polished and etched with 2% nital to reveal the microstructure. For both one-step and two-step, the microstructures were obtained using a scanning electron microscope (SEM).
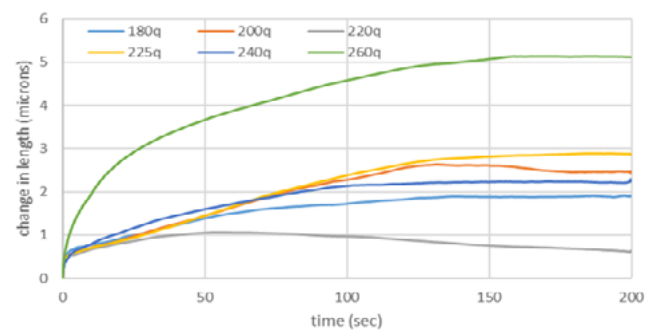
Figure 2: Dilation in samples at the partitioning temperature of 400 °C after quenched at different temperatures above and below optimum quench temperature of 225 °C

3. Results

3.1 Two-step Q&P heat treatment

In two-step Q&P heat treatment, optimum quench temperature was calculated using Speer Model.[2] The optimum quench temperature for the alloy used was calculated as 225°C and is described in.[9] The sample length change in the specimen was analyzed from the start to the end of the partitioning process. The dilation during the isothermal hold at different quench temperatures is shown in Figure 2. The dilation observed during the partitioning step is related to carbon partitioning from martensite to the austenite phase, bainite formation, or growth of the martensite phase. At low quench temperatures 200 and 220°C, rapid expansion was observed, followed by a contraction. In the 240°C quench after the initial expansion, there was a gradual rise before leveling off. In the case of a 260°C quench, a significant increase in length related to bainite formation was observed, as carbon partitioning alone could not lead to such an increase in dilation.

3.2 Isothermal or One-step Q&P treatment

In one-step Q&P heat treatment, the isothermal hold after quenching was for 600 s. At temperatures far below M_s, i.e., 215i and 225i curves in Figure 3, there was a rapid expansion for 100 s, and in the latter part of the hold, there was a slight expansion, but the curve saturated towards the end of the hold time. This initial expansion was attributed to the carbon partitioning from the athermal martensite to RA. For 400i and 425i curves, the expansion was
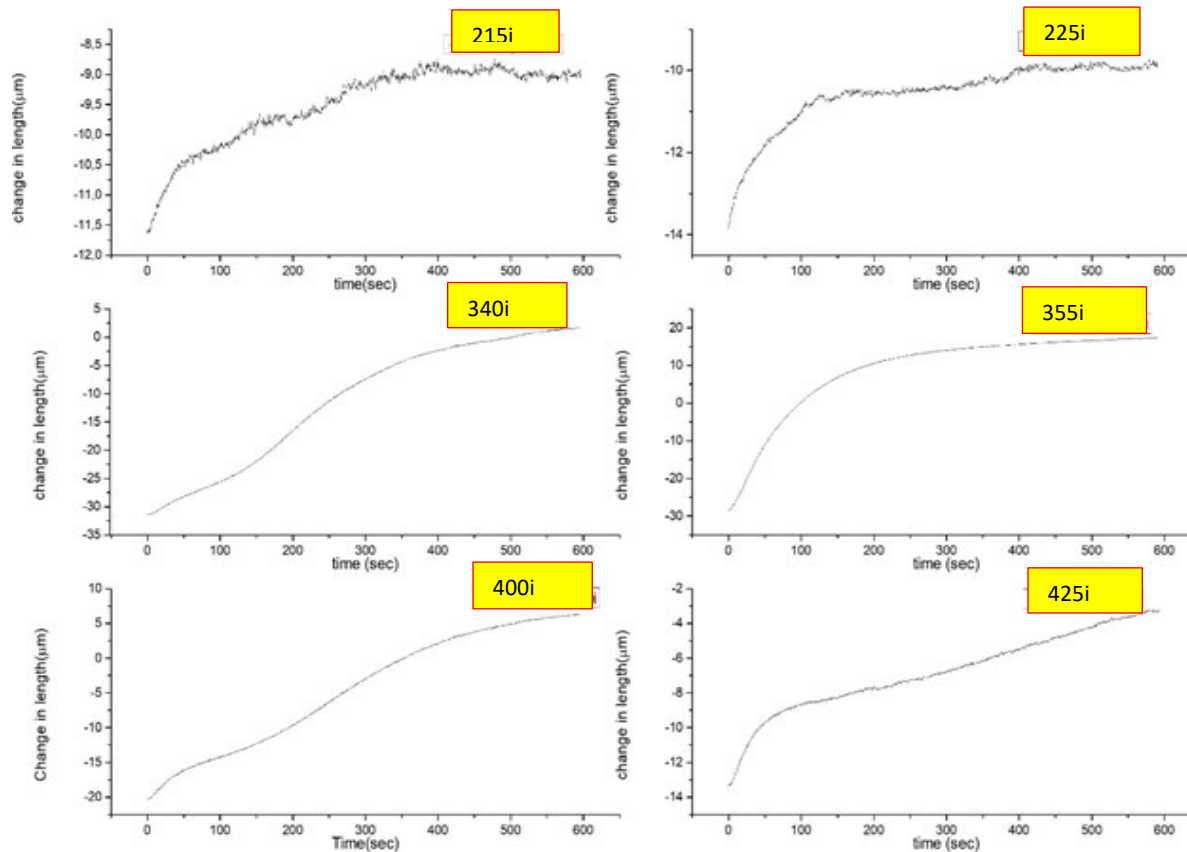
Figure 3: Change in length during isothermal hold after quenching at 215 and 225 C(below Ms), 340 and 355°C (near Ms), and 400 and 425°C(above Ms)

recorded with no saturation as the hold time increased, signifying incomplete reaction.

The raw data obtained for each isothermal reaction during different holding times were subjected to cubic spline interpolation to get a fixed incremental time interval value. The data was later smoothed by moving average to decrease the scatter. Assuming that the JMAK equation could be fitted into the data set, the values of n and k were obtained from the plot of $\ln \left(\ln \left(\frac{1}{1-f_{\alpha'}} \right) \right)$ *vs Int*. The model's fit for isothermal transformations of 215i and 225i (way below M_s), 340i and 355i (near M_s), and 400i above M_s are presented in Figure 4. The results indicate a good fit below and near M_s temperatures.

3.3 Neutron diffraction

The phase analysis using the data from neutron diffraction is obtained by the Rietveld method. Results of phase analysis for both one and two-step Q&P heat treatment are presented in Table

2. The carbon in RA was obtained from equation 2 using the lattice parameter of the RA obtained from neutron diffraction.

The data analysis shows the RA amount increased with an increase in quench temperature in two-step Q&P heat-treatment. Maximum RA was expected at 225°C quench as per Speer model,[2] but it was found at 260°C with a volume fraction of 22%. The carbon content in RA also decreased 0.65 to 045 wt% C with an increase in quench temperature. In one step Q&P heat-treatment, the amount of RA also increased up to 355°C, which is below the M_s temperature(368°C), and then above M_s, it decreased with an increase in temperature. Above the M_s, the RA was not stabilized after 600 s during the isothermal hold, and the austenite transformed martensite on quenching to room temperature. The carbon content in RA also followed the same trend, i.e., increased with an increase in the isothermal hold temperature up to near the M_s and decreased beyond the Ms temperature.

Table 2: Retained austenite and its carbon content in one-step and two-step Q&P heat-treatment at various quench temperatures

Two-step Q&P heat treatment			One-step Q&P heat treatment		
Quench temperature(°C)	%RA	%C in RA	Quench temperature(°C)	%RA	%C in RA
180	10.27	0.66	215	6,14	0,049
200	13.03	0.59	225	6,32	0,11
220	13.65	0.59	340	15,14	0,35
225	14.75	0.57	355	19	0,354
240	17.74	0.51	400	17,09	0,34
260	22.27	0.46	425	6,31	0,13
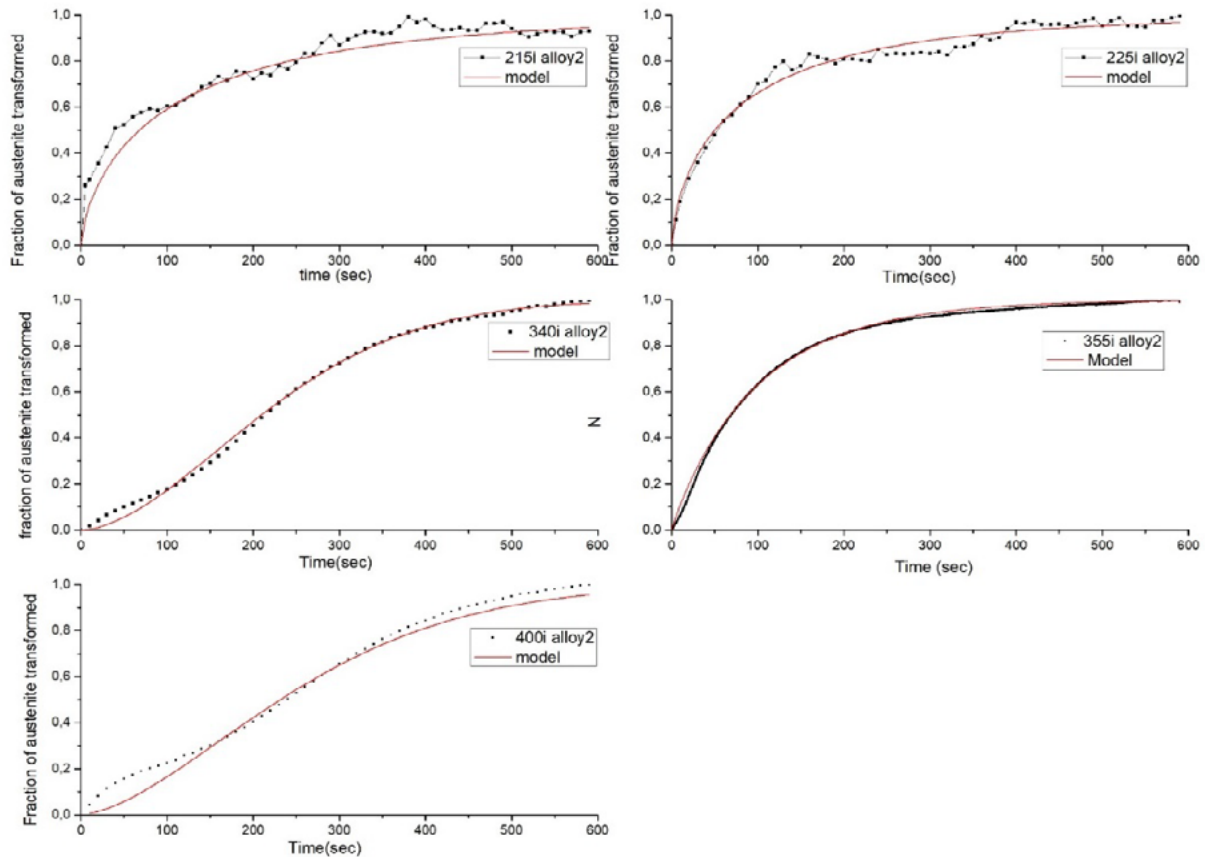
Figure 4: Fraction of austenite transformed during the isothermal holding for the time of 600s along with JMAK model applied to samples isothermally held at 215 and 225°C(way below M_s), 340 and 355°C (near M_s), and 400°C above M_s

3.4 Microstructures

The microstructures of both the two-step and one-step Q&P heat treatment are presented for the two quench temperatures of 220 and 260°C and 215 and 355°C, respectively, based on the lowest and highest RA identified by neutron diffraction. For the two-step quench, the microstructures show wedge-shaped lath with carbides and few laths with no carbides, which are unetched. The 260°C sample showed the presence of bainite. The RA could not be identified using the normal secondary electron imaging (SEI) but using electron back-scattered diffraction (EBSD).[9] As may be seen in Fig 5, the lath size increased as the quench temperature increased. The unetched laths have two different morphology (i) thin and long ridge shaped (ii) polygonal-shaped structure.

The one-step Q&P heat treatment at 215°C showed elongated lath with carbide precipitated in it, as seen in Figure 6. It also showed the presence of unetched coarse, mainly wedge-shaped lath, which could be newly formed martensite (SM) after quenching to room temperature. The martensite formed after the second quench has a high carbon content, so it was not etched easily with nital. The
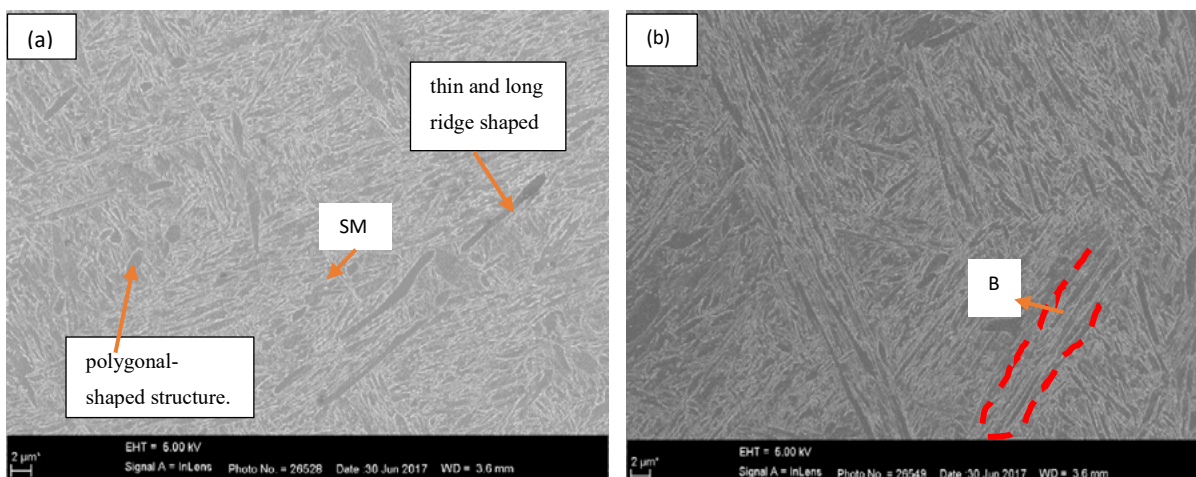
Figure 5: Microstructure of samples after two-step Q&P heat treatment with quenching (a) 220°C (b) 260°C and after partitioning at 400 °C.(B is bainite; SM secondary martensite)
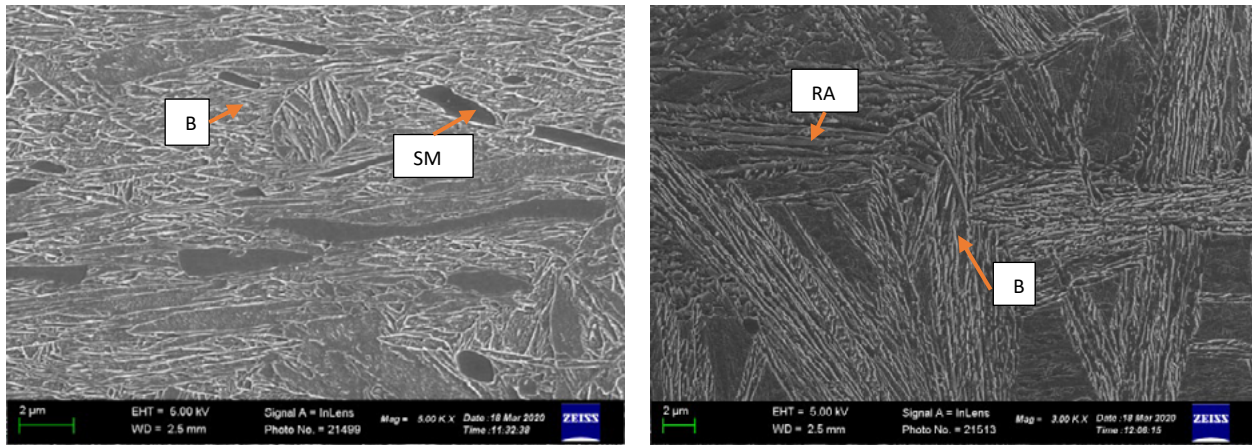
Figure 6: Microstructure of samples after the one-step Q&P heat treatment with quenching (a) 215 °C (b) 355 °C (B=Bainite RA= Retained austenite SM=Secondary martensite)

355°C shows a different morphology of laths, which indicates the formation of bainite along with martensite and retained austenite.

4. Discussion

The transformation during the partitioning stage of one and two-step Q&P was analyzed by dilatometry. The phase transformations are represented as a time-dependent change in length, Figs 2 and 3. For the two-step, Q&P process, below the optimum quench temperature of 225 °C, a rapid rise in length was initially seen in Figure 2. Santofimia et al.[10] had calculated the volume change associated with carbon partitioning. The small rapid rise initially seen is attributed to carbon partitioning, as suggested by Santofimia et al.[10] The magnitude of length change differs slightly for all quench temperatures except for the 260°C quench, where the extent of change is large. This implies a different transformation product during the partitioning stage. At lower quench temperatures of 180 and 200°C, the primary martensite formed undergoes tempering, leading to the contraction observed in Figure 2 in the later partitioning stage. Onink et al.[11] had related the contraction to the decomposition of austenite films saturated with carbon into carbon depleted austenite and cementite. Above the optimum quench temperature, no contraction was observed as the carbon partitioning was balanced by tempering of martensite. At 260°C, where RA was found to be maximum, there was evidence of the bainite formation, Figure 5(b). The bainite formation led to the rejection of carbon from the ferrite plate, thereby enriching the surrounding austenite and stabilizing it.

There was an increase in length over time during the isothermal hold stage in one-step Q&P heat treatment. However, the dilation profile differed for the sample quenched above and below the M_s temperatures. Above M_s temperature, the initial structure present was austenite, and there was initial rapid expansion followed by gradual expansion. This implied that the transformation did not undergo completion even after 600 seconds of isothermal hold. Below M_s, the initial expansion was followed by saturation after 200 seconds except for the sample held at 340°C. The sample held at 355°C showed the highest magnitude of length change and exhibited the maximum RA (19%) for the one-step Q&P process. This was further investigated with JMAK modeling of the curves, TTT diagram, and microstructural examination. From the JMAK model fit, the "n" and "k" parameters were evaluated and plotted as a function of temperature in Fig 7.

The sharp change in "n" and "k" values around the M_s indicate the decomposition product from austenite above and below M_s is different. The TTT diagram obtained from the isothermal transformation regime shows a "swing back effect" just below the Ms, Fig 8. According to Oka et al.[12] and Radcliffe et[13] swing back phenomenon is related to the presence of thin plates of martensite, which accelerates the nucleation of bainite in the adjacent RA. This leads to carbon transfer into austenite, leading to its stabilization. Observation of microstructures at 355°C Figure 6(b) revealed the presence of bainite. This is why a high amount of RA was observed at 355°C quenched sample in one step Q&P.
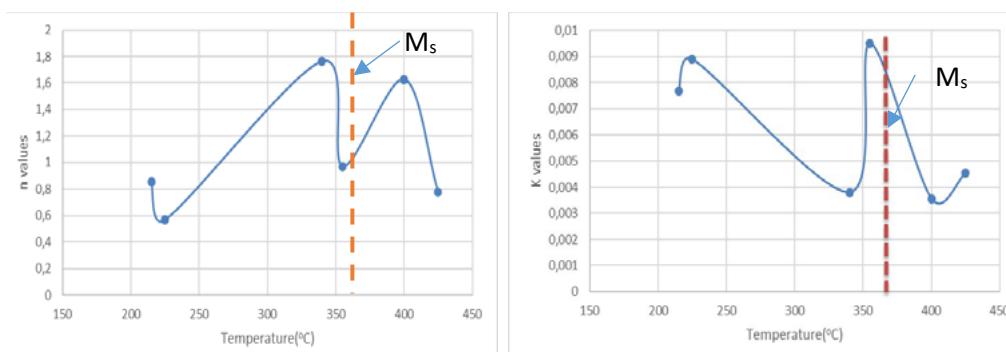
Figure 7: Variation of JMAK parameters (a) "n" and (b) "k" as a function of quench temperatures during one-step Q&P heat treatment
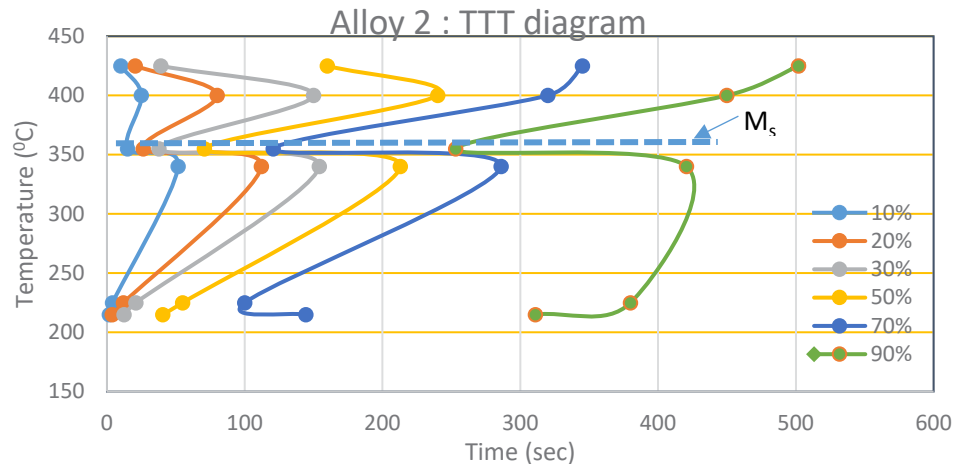
Figure 8: TTT diagram for isothermal hold at various quench temperatures shows the "swing back" effect below Ms for one-step Q&P

The RA content is necessary to enhance ductility in Q&P steels, and therefore, the two-step Q&P heat treatment seems to be a better option based on the neutron diffraction results. The carbon content in the RA is higher than the one-step Q&P process, which should enhance the stability of RA. In the partitioning stage, carbon atoms from primary martensite and freshly formed isothermal transformation products partition to untransformed austenite. The kinetics of carbon atom transfer becomes slower as the austenite is continuously get reduced. This explains a lower amount of the RA is observed at lower quench temperatures, i.e., way below M_s. At temperature above, M_s austenite was not stabilized as evidenced from neutron diffraction results. This is because there was no supersaturated martensite from where carbon could partition. In terms of microstructure one-step, Q&P heat-treated sample exhibited a coarser lath structure than the two-step Q&P one due to the growth of laths during the isothermal hold, where the time of hold was larger.

5. Conclusion

The study of one-step and two-step Q&P heat treatments on a medium carbon high silicon alloy using dilatometry was carried out, and the following conclusions can be made:

- The two-step Q&P process gives higher amounts of the RA than the one-step Q&P process; hence the two-step process is preferable due to enhanced kinetics regarding stabilization and a finer microstructure.

- The "n" and "k" parameters in the JMAK equation revealed the kinetics of austenite decomposition to be different above and below M_s. in one-step Q&P process

- Below the M_s, the presence of thin martensite plates accelerated the transformation of the RA to bainite which was evident from the "swing-back" in TTT the diagram

References

1. Fonstein N. Advanced high strength sheet steels : physical metallurgy, Design, Processing, and Properties. Springer; 2015. 393 p.
2. Speer J, Matlock DK, De Cooman BC, Schroth JG. Carbon partitioning into austenite after martensite transformation. Acta Mater. 2003;51(9):2611–22.
3. Barbe; L, Verbeken K, Wettinck E. Effect of the Addition of P on the Mechanical Properties of Low Alloyed TRIP Steels. ISIJ Int. 2006;46(8):1251–7.
4. Speer JG, Matlock D, DeCooman BC, Schroth JG. Comments on "On the definitions of paraequilibrium and orthoequilibrium" by M. Hillert and J. Ågren, Scripta Materialia, 50, 697–9 (2004). Vol. 52, Scripta Materialia. 2005. 83–85 p.
5. S.J. Kim, H.S. Kim, and B.C.D.Cooman.: Nelson BD, editor. AIST Steel Properties and Applications Conference Proceedings. Detroit: MS&T'07; 2007. p. 73–83.
6. Kim DH, Speer JG, Kim HS, De Cooman BC. Observation of an Isothermal Transformation during Quenching and Partitioning Processing. Metall Mater Trans A 2009;40(9):2048–60.
7. David WIF. Powder diffraction: Least-squares and beyond. J Res Natl Inst Stand Technol. 2004;109(1):107.
8. van Dijk NH, Butt AM, Zhao L, Sietsma J, Offerman SE, Wright JP, et al. Thermal stability of retained austenite in TRIP steels studied by synchrotron X-ray diffraction during cooling. Acta Mater. 2005;53(20):5439–47.
9. Kurup V, Siyasiya CW, Mostert RJ. Effect of the quench temperature on the mechanical properties of a medium C Mn high Si steel during Q&P heat-treatment process. IOP Conf Ser Mater Sci Eng 2019;655:12002.
10. Santofimia MJ, Zhao L, Sietsma J. Volume Change Associated to Carbon Partitioning from Martensite to Austenite [Internet]. Vols. 706–709, Materials Science Forum. 2012. p. 2290–5.
11. Onink M, Brakman CM, Tichelaar FD, Mittemeijer EJ, van der Zwaag S, Root JH, et al. The lattice parameters of austenite and ferrite in Fe3C alloys as functions of carbon concentration and temperature. Scr Metall Mater. 1993;29(8):1011–6.
12. Oka M, Okamoto H, Ishida K. Transformation of lower bainite in hypereutectoid steels. Metall Trans A 1990;21(3):845–51.
13. Radcliffe S V, Rollason EC. The kinetics of the formation of bainite in high-purity iron-carbon alloys. J Iron Steel Inst. 1959;191:56–65.